

Article

Not peer-reviewed version

Wheelset Wear Condition Evaluation Based on High-precision Online Measurement of Geometric Parameters

[Saisai Liu](#), [Qixin He](#), [Wenjie Fu](#), Qiang Han, [Qibo Feng](#)*

Posted Date: 17 March 2026

doi: 10.20944/preprints202603.1316.v1

Keywords: wheel wear measurement; wear condition evaluation; multi-dimensional sensors fusion; matter-element evaluation model; train wheel wear



Preprints.org is a free multidisciplinary platform providing preprint service that is dedicated to making early versions of research outputs permanently available and citable. Preprints posted at Preprints.org appear in Web of Science, Crossref, Google Scholar, Scilit, Europe PMC.

Copyright: This open access article is published under a [Creative Commons CC BY 4.0 license](#), which permit the free download, distribution, and reuse, provided that the author and preprint are cited in any reuse.

Disclaimer/Publisher's Note: The statements, opinions, and data contained in all publications are solely those of the individual author(s) and contributor(s) and not of MDPI and/or the editor(s). MDPI and/or the editor(s) disclaim responsibility for any injury to people or property resulting from any ideas, methods, instructions, or products referred to in the content.

Article

Wheelset Wear Condition Evaluation Based on High-Precision Online Measurement of Geometric Parameters

Saisai Liu ^{1,2}, Qixin He ^{1,2}, Wenjie Fu ^{1,2}, Qiang Han ³ and Qibo Feng ^{1,2,*}

¹ A School of Physical Science and Engineering, Beijing Jiaotong University, Beijing 100044, China

² MOE Key Laboratory of Luminescence and Optical Information, Beijing Jiaotong University, Beijing 100044, China

³ Infrastructure Inspection Research Institute, China Academy of Railway Sciences Corporation Limited, Beijing 100081, China

* Correspondence: qbfeng@bjtu.edu.cn; Tel.: +86-010-51685558

Abstract

Train wheel wear is a critical factor affecting train operational safety, making the accurate and objective evaluation of wheel wear condition essential. However, current approaches are still constrained by inadequate measurement accuracy and incomplete evaluation methods, to address this issue, this study proposes an integrated method for the high-precision measurement and wear condition evaluation of train wheels. A multi-sensor data fusion-based measurement method is developed to synchronously acquire key wear-related parameters, including wheel diameter, flange height, and flange thickness. Based on the measured data, an improved matter-element model combined with game-theoretic weighting is established to evaluate wheel wear condition. Experimental results show that the proposed online measurement method for in-service wheels achieves standard deviations below 0.15 mm, and the measurement errors satisfy the requirements of Chinese railway industry standards. The evaluation results derived from the high-precision measurement data indicate that wheel wear condition gradually deteriorates with increasing service mileage, and that flange height wear is the dominant factor affecting the wear grade. These findings are consistent with actual operating conditions. The proposed method integrates high-precision multi-parameter measurement with wear condition evaluation, providing a reliable technical basis for wheel condition monitoring and predictive maintenance in rail transit.

Keywords: wheel wear measurement; wear condition evaluation; multi-dimensional sensors fusion; matter-element evaluation model; train wheel wear

1. Introduction

As the core load-bearing component connecting trains and tracks, the wear condition of train wheels directly determines the safety, stability, and comfort of train operation. Excessive wheel wear will aggravate wheel-rail contact fatigue and even cause serious safety accidents such as derailment. Therefore, the accurate evaluation of wheel wear condition is of great importance for train operation safety, which requires the evaluation model to be effective and accurate, and in turn relies on high-precision wear measurement data as the support. Thus, effective, accurate evaluation and high-precision measurement are both key research directions in the fields of railway transportation and metrology [1–3].

For the accurate evaluation of wheel wear, the effectiveness and accuracy of the evaluation model are critical. However, most existing studies rely on the threshold judgment of a single indicator such as diameter or flange thickness, which cannot fully reflect the overall wear and potential risks, and research on multi-indicators comprehensive evaluation is relatively insufficient. In recent years,

the matter-element evaluation method and combined weighting method have exhibited significant advantages in multi-indicators comprehensive evaluation [4–6], and have been maturely applied in many fields such as rail transit [7–9], civil engineering [10], geotechnical engineering [11], and hydraulic engineering [12]. The matter-element evaluation method is used to handle the fuzziness and uncertainty in the evaluation process, making the evaluation results more intuitive and reliable. Yi et al. [7] constructed a catenary condition evaluation model, using the matter-element model to determine the catenary condition grade, in which EWM and AHP were used to determine the indicators weights. Peng et al. [13] constructed a rail transit planning scheme based on the matter-element model, in which subjective and objective weights were used for comprehensive weighting of evaluation indicators. Up to now, no research has introduced the matter-element evaluation method into the comprehensive evaluation of train wheel wear, leaving an obvious research gap.

On the other hand, the accuracy of evaluation results depends entirely on the quality of measurement data, which means high-precision wheel wear measurement is the prerequisite for effective and accurate evaluation. Ran et al. [14] proposed a wheel profile parameter measurement method based on line structured light vision sensing, and designed a targeted sub-pixel stripe center extraction algorithm to achieve fast and accurate measurement of wheel profiles. Pan et al. [15] adopted two sets of line structured light vision sensors for data compensation, improving the stability of profile measurement. Zheng et al. [16] constructed an on-line wheel diameter measurement system based on the three-point method. However, most existing measurement systems are difficult to realize synchronous high-precision measurement of wheel diameter and profile; in addition, coupled measurement errors between wheel diameter and profile are likely to be introduced during the measurement process, which fails to meet the requirements of multi-indicators comprehensive evaluation in terms of measurement accuracy, efficiency, and stability.

In this context, to solve the problems of inadequate wheel wear evaluation and insufficient measurement accuracy, this paper carries out systematic research on the measurement and evaluation of train wheel wear. Firstly, a multi-indicators comprehensive evaluation model for wheel wear based on game theory combined weighting and matter-element model is constructed. Secondly, a measurement method based on multi-dimensional sensor fusion is proposed to realize synchronous and accurate measurement of wheel wear and wheel diameter. Finally, experiments are carried out to verify the effectiveness of the measurement method and the accuracy of the evaluation model.

2. Comprehensive Evaluation Method of Train Wheel Wear

2.1. Indicator Selection and Overall Evaluation Flow

Based on existing research on wheel wear measurement[17–19] and vehicle dynamics analysis [20–22], three core indicators are selected to evaluate the wheel wear condition including wheel tread wear parameters flange height (FH), flange thickness (FT) and wheel diameter (D). These indicators are closely related to the safety and stability of train operation and they can directly reflect the overall wear degree of train wheels. Meanwhile they are accessible via wayside monitoring systems which ensures the engineering operability of the subsequent evaluation work.

The overall evaluation process of wheel wear condition as shown in Figure 1 consists of the following key steps.

First the evaluation indicators are determined. Combined with the actual requirements of wheel wear evaluation and existing research results the core indicators FH, FT, and D are selected to form an effective evaluation indicator system.

Second the comprehensive weights of the evaluation indicators are calculated. Specifically, the Analytic Hierarchy Process (AHP) is adopted to calculate subjective weights. The Entropy Weight Method (EWM) is used to calculate objective weights. Finally, the comprehensive weights of each indicator are obtained through game theory which balances the advantages of subjective and objective weighting methods.

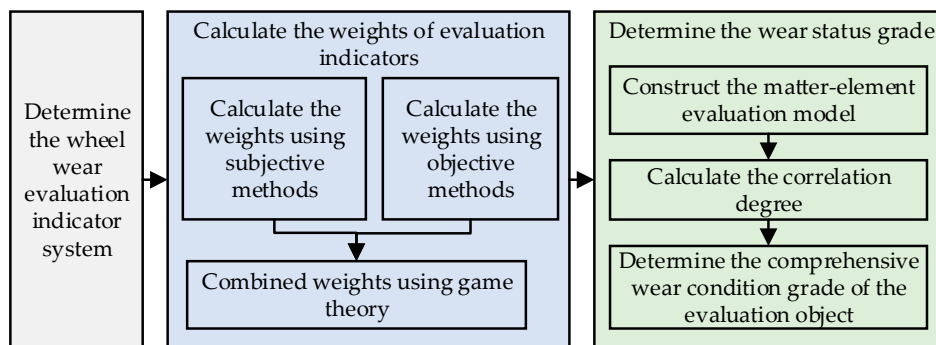


Figure 1. Overall evaluation flow of the train wheel wear comprehensive evaluation method.

Finally, the matter element evaluation model is constructed. The comprehensive correlation degree between the evaluated wheel and the preset wear condition grades is calculated through this model. Then the wear condition grade of the evaluated wheel is determined in accordance with the maximum membership principle.

2.2. Determination of Evaluation Indicator Weights

2.2.1. Subjective Weighting Based on AHP

AHP is a classic subjective weighting method that converts qualitative judgments of indicator importance into quantitative analysis, thereby solving the difficulty in directly quantifying the relative importance of wheel wear evaluation indicators and achieving more reasonable and reliable subjective weight distribution [23–25]. The key procedures for calculating subjective weights via the AHP are summarized as follows:

First, a judgment matrix is constructed by comparing the importance of each pair of indicators based on the 1–9 scale method [26]. The matrix is denoted as $A = (a_{ij})_{n \times n}$, where a_{ij} represents the importance of the i -th indicator relative to the j -th indicator, n is the number of indicators, and a_{ij} and a_{ji} are reciprocals of each other.

Second, the geometric mean of each row in the judgment matrix is calculated and normalized to obtain the subjective weight vector $w_{AHP} = (w_1, w_2, \dots, w_n)$.

Finally, a consistency check is conducted by computing the consistency ratio CR to verify the logical rationality of the judgment matrix. The matrix is considered acceptable only if $CR < 0.1$; otherwise, the matrix elements need to be revised [27].

2.2.2. Objective Weighting Based on EWM

EWM is a data-driven objective weighting approach that determines indicator weights based on the degree of data dispersion, where a higher degree of dispersion corresponds to a smaller entropy value and thus a higher indicator weight, indicating a greater impact on the evaluation objective [4,25,28]. The key steps for calculating objective weights using the EWM are detailed as follows:

First, data normalization is performed to eliminate differences in dimensions and orders of magnitude among different indicators.

Second, the entropy value e_j of each indicator is calculated.

$$e_j = -\left(\sum_{i=1}^m f_{ij} \ln f_{ij}\right) / \ln m, \quad (1)$$

$$f_{ij} = y_{ij} / \sum_{i=1}^m y_{ij}, \quad (2)$$

where m represents the number of samples, f_{ij} represents the contribution of the i -th sample to the j -th indicator, y_{ij} denotes the normalized value.

Finally, the weight of each evaluation indicator is calculated; the weight is negatively correlated with the entropy value, meaning that indicators with smaller entropy values (higher data dispersion) are assigned higher weights.

$$w_{EWM} = (1 - e_j) / \sum_{j=1}^n (1 - e_j), \quad (3)$$

2.2.3. Combined Weights Based on Game Theory

To balance the advantages of subjective and objective weights and avoid the limitations of single weighting methods, the game theory is applied to combine the weight vectors w_{AHP} and w_{EWM} calculated in the previous two sections. This method determines the optimal combination coefficients through game theory optimization, ensuring that the combined weights are effective, reasonable [7,9,25]. The key steps for calculating objective weights using the EWM are detailed as follows:

First, the game theory optimization objective function is constructed. The objective function is established based on the principle of minimum Euclidean distance between the combined weight and the two single weight vectors. The core goal is to minimize the deviation between the combined weight vector and the subjective and objective weight vectors.

$$\min \left\| \sum_{l=1}^2 a_l \cdot w_l - w_k \right\|_2, \quad (4)$$

where a_l represent the combination coefficients corresponding to the weight vector w_l respectively.

Second, according to the matrix differential theory, derive the constraint conditions for the optimal combination coefficient vector $a = [a_1, a_2]^T$.

Finally, the combined weights are calculated. The obtained combination coefficient vector a is normalized, and then the normalized combination coefficients are multiplied by the corresponding subjective and objective weight vectors respectively and summed to obtain the final comprehensive combined weight vector w for each evaluation indicator.

2.3. Matter-Element Evaluation Model

The matter-element evaluation model is a comprehensive evaluation method based on matter-element analysis, which accurately and intuitively determines the wear condition grades of wheel in combination with the above comprehensive weights [6,11,13].

2.3.1. Determination of Matter-Element Matrix, Classical Domain, and Joint Domain

The matter-element matrix is used to describe the evaluated object comprehensively, which expresses the evaluated wheel (denoted as N), its evaluation indicators (denoted as c) and the measured values of indicators (denoted as v) in a unified form, defined as $R = [N, c, v]$. Here, N represents the wheel to be evaluated, c corresponds to the core evaluation indicators (such as. FH, FT, and D), and v is the actual measured value of each indicator.

The classical domain refers to the value range of each evaluation indicator when the evaluated wheel belongs to a specific wear grade (e.g., excellent, qualified, critical, unqualified). It is defined as $R_{oj} = [N_{oj}, c_i, x_{oij}]$, where N_{oj} denotes the j -th wear grade, c_i represents the i -th evaluation indicator, and x_{oij} is the value range of the i -th indicator corresponding to the j -th wear grade.

$$R_{oj} = \begin{bmatrix} N_{oj} & c_1 & x_{o1j} \\ & c_2 & x_{o2j} \\ & c_3 & x_{o3j} \end{bmatrix} = \begin{bmatrix} N_{oj} & c_1 & (a_{o1j}, b_{o1j}) \\ & c_2 & (a_{o2j}, b_{o2j}) \\ & c_3 & (a_{o3j}, b_{o3j}) \end{bmatrix} \quad (5)$$

The joint domain refers to the maximum possible value range of each evaluation indicator, which covers all possible values of the indicators in the classical domain and other potential value ranges. It is defined as $R_p = [N_p, c_i, x_{pi}]$, where N_p denotes the set of all possible wear condition of the wheel, and x_{pi} is the maximum possible value range of the i -th evaluation indicator.

$$R_{pj} = \begin{bmatrix} N_p & c_1 & x_{p1} \\ & c_2 & x_{p2} \\ & c_3 & x_{p3} \end{bmatrix} = \begin{bmatrix} N_{pj} & c_1 & (a_{p1}, b_{p1}) \\ & c_2 & (a_{p2}, b_{p2}) \\ & c_3 & (a_{p3}, b_{p3}) \end{bmatrix} \quad (6)$$

2.3.2. Calculation of Indicator Correlation Degree

The correlation degree is employed to quantitatively measure the relevance between each indicator value of the evaluated wheel and each predefined wear grade, which is calculated based on the distance between the indicator value and the corresponding classical domain range.

$$k_{ij} = \begin{cases} 1 - \rho(v_{ij}, x_{oij}) / |x_{oij}| & v_i \in x_{oij} \\ -\rho(v_{ij}, x_{oij}) / |x_{pi}| & v_i \notin x_{oij} \end{cases} \quad (7)$$

$$\rho(v, x) = |v - x_0|, \quad (8)$$

where ρ represents the distance between the indicator value and the classical domain. Let v be the indicator value, x the classical domain, and x_0 the optimal value in the classical domain. For decreasing-type indicators such as D and Sd, x_0 is taken as the upper bound of the classical domain; for increasing-type indicators such as FH, x_0 is taken as the lower bound of the classical domain.

2.3.3. Calculation of Comprehensive Correlation Degree and Wear Grade Determination

The comprehensive correlation degree $K_j(N)$ is calculated via the linear weighted summation of the correlation degree k_{ij} of each indicator and its corresponding weight w_i .

$$K_j(N) = \sum_{i=1}^3 w_i k_{ij} \quad (9)$$

where, $K_j(N)$ denotes the comprehensive correlation degree of the evaluated wheel N with respect to the j -th wear grade, k_{ij} represents the correlation degree of the i -th indicator corresponding to the j -th wear grade, and w_i stands for the weight of the i -th indicator.

3. High-Precision Wheel Wear Measurement Method and System

To achieve simultaneous, high-accuracy online measurement of multiple key parameters that directly determine wheel wear condition, a novel measurement system fused with structured light vision sensors and displacement sensors is developed in this paper.

3.1. Definition of Wheel Wear Parameters

As shown in Figure 2, FH denotes the vertical distance from flange top point A to the datum point; FT refers to the horizontal distance from point B to the wheel inner side; D represents the rolling circle diameter at the datum point. As critical indicators for wheel wear condition evaluation, the accurate measurement of these parameters is essential for reliable condition assessment and timely maintenance.

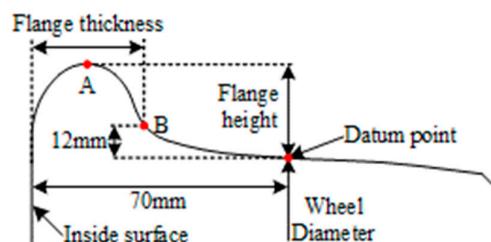


Figure 2. Definition of wheel wear parameters.

3.2. Wheel Wear Measurement Method

To achieve accurate and reliable measurement of the key parameters, a multi-sensor fused online measurement system is developed in this study. The system design fully combines the complementary advantages of different sensing technologies. On the one hand, laser displacement sensors (LDS) feature high precision in large-range dimensional measurement and displacement measurement, which are suitable for wheel diameter measurement, but cannot obtain complete wheel profile information. On the other hand, line-structured light vision sensors (LSLVS) can reconstruct the full wheel profile effectively, but may suffer from eccentricity errors. Therefore, the synergistic fusion of LSLVS and LDS is adopted in the system design, and the data fusion is implemented in the algorithm flow to suppress measurement errors and improve overall accuracy. The proposed system is mainly composed of a sensor measurement unit, a position trigger unit, a data processing unit, and a circuit driving unit. To ensure the consistency of wear information acquired by multiple sensors and achieve high-precision measurement based on sensor fusion, an integrated layout for multi-dimensional sensors is implemented, as illustrated in Figure 3a. Specifically, two LSLVSs are symmetrically arranged along the rail, projecting coplanar light planes along the wheel's radial direction to fully cover the tread. Meanwhile, three 1D LDS are installed outside the rail for tread scanning. As the wheel passes through the trigger unit, both types of sensors synchronously collect raw data: the LSLVS captures the light stripe images of the wheel's inner and outer contours, as shown in Figure 3b, while the LDS continuously acquires one-dimensional displacement data, as illustrated in Figure 3c. After the train passes, the sensor data are fused, and the key wear parameters are calculated to obtain the final evaluation results.

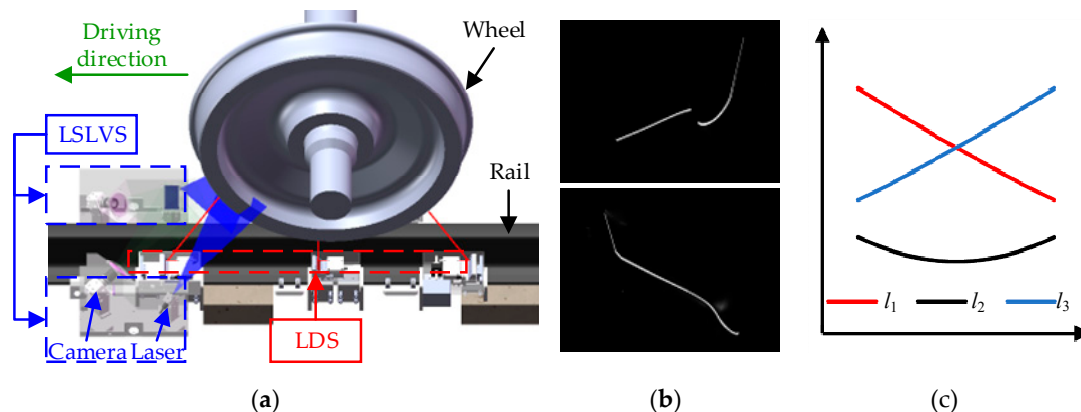


Figure 3. Sketch of wheel wear measurement system. (a) Sensor measurement unit; (b) 2D images captured by LSLVSs; (c) Distance acquired by 1D-LDSs.

3.3. Multi-Sensor Data Fusion

Based on the description of the measurement method, this section focuses on several key steps in multi-sensor data fusion measurement. First, the wheel wear parameters are initially calculated based on the measurement principle of the structured light vision sensor and the three-point diameter measurement principle. Subsequently, the core steps and mathematical model of data fusion are introduced.

3.3.1. Preliminary Calculation of Wear Parameters

The measurement principle of the structured light vision sensor is based on the camera imaging model and light plane geometric constraints, which converts two-dimensional pixel coordinates into a three-dimensional measurement contour, as shown in Figure 4a. $O_w-X_wY_wZ_w$ is defined as the world coordinate system; $O_{ci}-X_{ci}Y_{ci}Z_{ci}$ and $O_{co}-X_{co}Y_{co}Z_{co}$ denote the coordinate systems of the inner and outer cameras, respectively; $O_{ii}-X_{ii}Y_{ii}$ and $O_{io}-X_{io}Y_{io}$ are the image coordinate systems of

the corresponding cameras, respectively. For an arbitrary image point $pi(xi, yi)$ in the image, it can be reconstructed to the world coordinate system $Pw(Xw, Yw, Zw)$ by the Equation (10) [29–31]. After reconstructing the wheel profile coordinates, FH and FT are initially calculated according to the definitions of wear parameters illustrated in Figure 2.

$$\begin{cases} aXc + bYc + cZc + d = 0 \\ Zc(xi, yi, 1)^T = McLc(Xw, Yw, Zw, 1)^T \end{cases} \quad (10)$$

where, (a, b, c, d) represent the coefficients of the light plane equation; Zc is a non-zero constant representing the scale factor; Mc denotes the camera intrinsic parameters; Lc represents the rigid transformation matrix of the camera coordinate system relative to the world coordinate system.

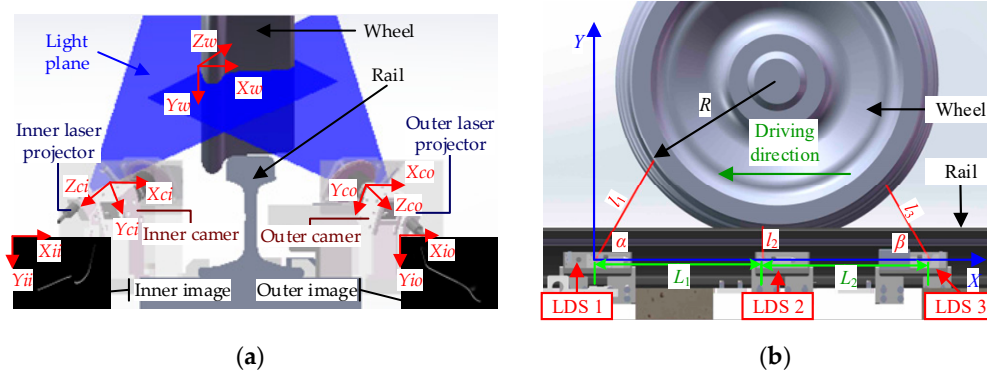


Figure 4. Principle of wheel wear measurement. (a) Principle of profile measurement; (b) Principle of diameter measurement.

The three-point diameter measurement principle is illustrated in Figure 4b. The emission angles of the two LDS sensors are defined as α and β , and their distances to LDS 2 are L_1 and L_2 , respectively. A two-dimensional Cartesian coordinate system is established with the left one-dimensional laser displacement sensor (LDS 1) as the origin, where X denotes the rail direction and Y represents the direction perpendicular to the rail surface. As shown in Figure 3c. The minimum value of l_2 indicates that the wheel is located directly above LDS 2. At this moment, the diameter of the measured circle is calculated according to the Equation (11) [16].

$$D' = \frac{L_1^2 + l_1^2 + l_2^2 - 2L_1l_1\cos\alpha - 2l_1l_2\sin\alpha}{2l_1\sin\alpha - 2l_2} + \frac{L_2^2 + l_3^2 + l_2^2 - 2L_2l_3\cos\beta - 2l_3l_2\sin\beta}{2l_3\sin\beta - 2l_2} \quad (11)$$

3.3.2. Data Fusion Improves the Accuracy of Wear Calculation

The wheel diameter is defined as the circumference diameter at the datum point, as shown in in Figure 5a, which cannot be directly measured during train operation. The red arrows denote the emission light planes of the displacement sensors. Therefore, the diameter D' calculated by Equation (11) is not the actual wheel diameter, but the circumference diameter at point P on the wheel tread. To obtain an accurate wheel diameter, further correction is required based on the profile coordinates reconstructed by the LSLVS. Thus, the actual wheel diameter D is determined using the compensation model given in Equation (12).

$$D = D' + 2\Delta r, \quad (12)$$

where Δr is calculated from the reconstructed wheel profile.

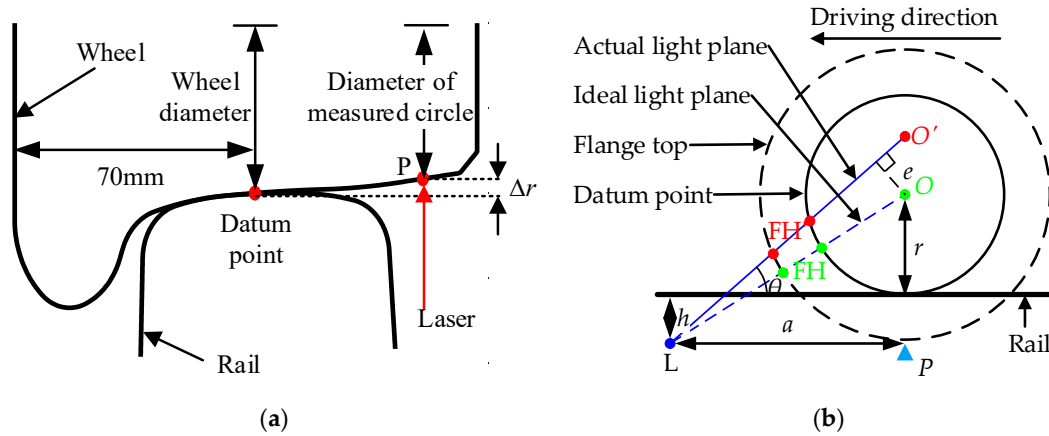


Figure 5. Calculation principle of wheel wear. (a) Principle of diameter calculation; (b) Principle of profile calculation.

The mathematical model for profile measurement using the vision sensor is established based on a standard wheel, as illustrated in Figure 5b. The laser L is mounted at a height h below the rail surface, and the angle between the light plane and the rail surface is θ . To ensure the light plane passes through the axle O for accurate wheel profile measurement, the trigger position P is set at a horizontal distance a from the laser, which strictly determines the moment of image capture by the camera. At this trigger instant, the light plane intersects the flange top and the datum point at points F and H , respectively, where FH corresponds to the nominal flange height of the measured wheel. However, owing to the varying diameters of actual in-service wheels, fixed trigger timing cannot guarantee that the light plane remains at the optimal position in all acquired profile images. In this case, the vertical deviation between the light plane and the actual axle is defined as e , and the measured flange height is denoted as FH' . The unknown wheel diameter introduces profile distortion and degrades the accuracy of high-precision online profile measurement using only the vision sensor, which cannot compensate for such distortion.

To improve the measurement accuracy of wheel wear, the wheel diameter initially calculated by the 1D LDSs is adopted to correct the eccentricity error. Based on the geometric constraints of right triangles, the expression for the corrected true FH can be further calculated by Equation (13), and the expression for the eccentricity distance e can be derived by Equation (14).

$$FH = \sqrt{(FH' + \sqrt{r^2 - e^2})^2 + e^2} - r, \quad (13)$$

$$e = (a \tan \theta - r - h) \cos \theta, \quad (14)$$

where, r is the radius of the wheel to be measured. In the multi-sensor data fusion algorithm, the tread profile reconstructed by the LSLVS and the wheel diameter measured by the LDS are mutually compensated and calibrated to improve measurement accuracy. This approach addresses the coupled deviation problem in profile and diameter measurement that cannot be resolved by a single type of sensor, thereby achieving high-precision online measurement. To further enhance measurement accuracy, an iterative method is proposed. Specifically, the D is first estimated using Equations (11)–(12). Subsequently, high-precision profile parameters are obtained via Equations (13)–(14). Finally, the diameter correction and eccentricity compensation processes are performed iteratively, terminating when the variation in consecutive eccentricity distances e falls below 0.1 mm. Typically, two rounds of diameter correction and one round of profile correction are sufficient to meet the iterative requirements.

4. Experimental Verification

To verify the effectiveness and high precision of the proposed wheel wear measurement method and comprehensive evaluation model, experiments were designed and conducted. The experiments mainly focused on two aspects: verifying the measurement accuracy of the wheel wear parameters (FH, FT, and D) and validating the reliability of the matter-element evaluation model for wheel wear condition evaluation.

4.1. Experimental Verification of Wheel Wear Measurement

The system was deployed at the train depot entry section as shown in Figure 6 to evaluate the reliability of the proposed measurement method. Each LSLVS consisted of a line structured light laser with a wavelength of 405 nm, an industrial camera with a resolution of 1600×1200, and a fixed-focus lens with a focal length of 16 mm. The LSD had a sampling frequency of 1 kHz, with a resolution of 0.005 mm and an accuracy of 0.01 mm.

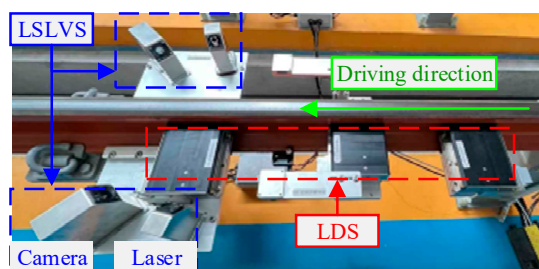


Figure 6. Physical diagram of the wheel wear measurement system.

To evaluate the stability of the proposed measurement system, online measurement experiments were performed on in-service train wheels. During the online field test, the train passed the measurement system at a constant speed of 5 km/h to conduct repeated measurements. Manual measurements were carried out 9 times on the tested wheels using the LLJ-4A detector and the digital wheel diameter gauge, and the averaged results were taken as reference values to verify the accuracy and repeatability of the system. The experimental results are presented in Table 1. The standard deviations (Std) of FH, FT, and D are 0.09, 0.13, and 0.14 mm, respectively; the mean absolute errors (MAE) are 0.15, 0.14, and 0.18 mm; and the maximum errors (ME) are 0.24, 0.34, and 0.36 mm. These results fully meet the accuracy requirements of China's railway industry for online measurement systems, i.e., ± 1.0 mm for D and ± 0.4 mm for FH and FT, which indicates that the proposed measurement system possesses high accuracy and favorable repeatability.

Table 1. Measurement results of a real train wheel (unit: mm).

Measurement number	FH	FT	D
1	27.80	32.58	914.49
2	27.78	32.42	914.58
3	27.84	32.45	914.71
4	27.84	32.70	914.79
5	27.67	32.36	914.44
6	27.78	32.55	914.86
7	27.63	32.42	914.79
8	27.58	32.74	914.64
Std	0.09	0.13	0.14
Mean	27.74	32.53	914.66
Manual	27.60	32.40	914.50

MAE	0.15	0.14	0.18
ME	0.24	0.34	0.36

4.2. Experimental Verification of Evaluation Model

To verify the reliability and effectiveness of the proposed wheel wear condition evaluation model, an in-depth analysis was conducted on the long-term monitoring data collected by the on-site measurement system. Installed at the railway operation site, the system continuously monitors train wheels passing through the measurement zone, with a practical measurement interval of approximately 15 days. A comprehensive evaluation was conducted on 8 sets of wear data obtained from the same wheel at different stages. These wheel wear datasets are sequentially labeled as L1, L2, ..., L8, and the corresponding detailed data are listed in Table 2.

Table 2. Measured values of wheel wear condition indicators (unit: mm).

Indicators	L1	L2	L3	L4	L5	L6	L7	L8
FH	27.16	27.42	27.45	27.72	28.05	28.49	28.76	28.95
FT	31.95	31.92	31.87	31.75	31.76	31.61	31.67	31.49
D	838.47	837.44	837.11	836.29	836.19	835.26	834.93	834.56

According to the railway industry specifications and practical application experience, the wheel wear condition was divided into four grades: Excellent, Qualified, Critical, and Unqualified. On this basis, the classical domain and joint domain of each wear evaluation indicator were determined. Finally, the weights of each indicator were calculated by adopting the weight calculation method described in Section 2.2. The detailed parameters of the joint domain, classical domain, and indicator weights are shown in Table 3.

Table 3. Joint domain, classical domain, and weights of wheel wear indicators.

Indicators	Joint domain (mm)	Classical domain (mm)				Weights		
		Excellent	Qualified	Critical	Unqualified	Subjective weights	Objective weights	Combined weights
FH	[27, 35]	[27, 29]	[29, 31]	[31, 33]	[33, 35]	0.1634	0.3304	0.2469
FT	[26, 32]	(30, 32]	(29, 30]	(28, 29]	[26, 28]	0.2970	0.3393	0.3181
D	[770, 840]	(800, 840]	(780, 800]	(775, 780]	[770, 775]	0.5396	0.3303	0.4349

Based on the determined classical domain, joint domain, and indicator weights, the indicator correlation degree of the wheel to be evaluated was calculated first, and then the comprehensive correlation degree was obtained through weighted summation. The calculation results of the indicator correlation degree and comprehensive correlation degree are shown in Table 4 and Table 5, respectively. To ensure the accuracy of the evaluation, the values are retained to 4 decimal places in accordance with common practice.

Table 4. Correlation of wheel wear condition indicators.

Sample number	Indicator correlation degree			
	Excellent	Qualified	Critical	Unqualified
L1	[0.9204, 0.9767, 0.9617]	[-0.1151, -0.3256, -0.0275]	[-0.2401, -0.4922, -0.1671]	[-0.3651, -0.3295, -0.1813]
L2	[0.7888, 0.9605, 0.9361]	[-0.0986, -0.3202, -0.0267]	[-0.2236, -0.4868, -0.1641]	[-0.3486, -0.3268, -0.1784]
L3	[0.7736, 0.9349, 0.9278]	[-0.0967, -0.3116, -0.0265]	[-0.2217, -0.4783, -0.1632]	[-0.3467, -0.3225, -0.1775]
L4	[0.6400, 0.8757, 0.9073]	[-0.0800, -0.2919, -0.0259]	[-0.2050, -0.4586, -0.1608]	[-0.3300, -0.3126, -0.1751]
L5	[0.4750, 0.8779, 0.9047]	[-0.0594, -0.2926, -0.0258]	[-0.1844, -0.4593, -0.1605]	[-0.3094, -0.3130, -0.1748]
L6	[0.2547, 0.8054, 0.8815]	[-0.0318, -0.2685, -0.0252]	[-0.1568, -0.4351, -0.1579]	[-0.2818, -0.3009, -0.1722]
L7	[0.1211, 0.8348, 0.8733]	[-0.0151, -0.2783, -0.0250]	[-0.1401, -0.4449, -0.1570]	[-0.2651, -0.3058, -0.1712]
L8	[0.0237, 0.7432, 0.8640]	[-0.0030, -0.2477, -0.0247]	[-0.1280, -0.4144, -0.1559]	[-0.2530, -0.2905, -0.1702]

Table 5. Comprehensive correlation of wheel wear condition.

Sample number	Comprehensive correlation degree				Max	Grade
	Excellent	Qualified	Critical	Unqualified		
L1	0.9563	-0.1439	-0.2885	-0.2738	0.9563	Excellent
L2	0.9075	-0.1378	-0.2815	-0.2676	0.9075	Excellent
L3	0.8920	-0.1346	-0.2779	-0.2654	0.8920	Excellent
L4	0.8313	-0.1239	-0.2665	-0.2571	0.8313	Excellent
L5	0.7901	-0.1190	-0.2615	-0.2520	0.7901	Excellent
L6	0.7025	-0.1042	-0.2458	-0.2402	0.7025	Excellent
L7	0.6753	-0.1031	-0.2444	-0.2372	0.6753	Excellent
L8	0.6181	-0.0903	-0.2312	-0.2289	0.6181	Excellent

It can be seen from Table 5 that the wheel was in the Excellent grade during the monitoring period of this stage. With the increase of operation mileage, the comprehensive correlation degree corresponding to the Excellent grade showed a gradual decreasing trend, indicating that the wear condition of the wheel gradually deteriorated as the operation mileage increased. Combined with Table 4, it can be further observed that the correlation degrees of FH, FT, and D with the excellent grade all decreased sequentially with the increase of measurement times, which was consistent with the change trend of the comprehensive correlation degree. Among them, the flange height indicator showed the most obvious downward trend in correlation degree, indicating that flange height wear is the key factor affecting the change of wheel wear grade, which is consistent with the actual railway operation law that wheel flange wear is the main form of wheel wear.

5. Conclusions

As the key load-bearing component connecting trains and tracks, wheel wear directly affects the safety, stability, and comfort of rail transit. To address the shortcomings of insufficient measurement accuracy and incomplete wear evaluation in conventional methods, this paper proposes an integrated framework for train wheel wear measurement and evaluation. A high-precision measurement method based on multi-sensor fusion is developed to realize synchronous measurement of FH, FT, and D. Meanwhile, an improved matter-element comprehensive evaluation model combined with game theory weighting is established for effective wear condition evaluation. Experimental results demonstrate that the proposed measurement method yields high precision and favorable repeatability in online measurement tests of train wheel. The Std of FH, FT, and D are 0.09, 0.13, and 0.14 mm, the MAE are 0.15, 0.14, and 0.18 mm, and the ME are 0.24, 0.34, and 0.36 mm, respectively. All of which are well within the accuracy specifications of China's railway industry for online measurement systems. Based on the monitoring values corresponding to different operating durations, the evaluation model was validated using 8 sets of wheel wear data measured at successive monitoring intervals. Comprehensive evaluation results demonstrate that the wheel remains at the Excellent grade during the monitoring period, while its comprehensive correlation degree gradually decreases, indicating a continuous deterioration of the wheel wear condition. Among all evaluation indices, the correlation degree of FH presents the most significant downward trend, revealing that flange height wear is the dominant factor governing the variation of wheel wear grade. This finding verifies that flange wear serves as the primary form of wheel wear, which is highly consistent with the actual field operation rules of railway vehicles. This work realizes the high-precision measurement and multi-indicators comprehensive evaluation of wheel wear, providing a technical solution for wheel condition monitoring and predictive maintenance, and further supporting the safe and stable operation of rail transit.

Author Contributions: Conceptualization and methodology, S.L. and Q.F.; software, S.L. and W.F.; validation, S.L. and Q.H.; investigation and data curation, S.L. and Q.H.; writing—original draft preparation, S.L.; writing—

review and editing, Q.F. and Q.H.; supervision, Q.F.; funding acquisition, Q.F. and Q.H. All authors have read and agreed to the published version of the manuscript..

Funding: This work was supported in part by the Beijing Natural Science Foundation under Grant 3262008 in part by the National Natural Science Foundation of China under Grant 51935002.

Data Availability Statement: Data underlying the results presented in this paper are not publicly available at this time but may be obtained from the authors upon reasonable request.

Conflicts of Interest: The authors declare no conflicts of interest.

References

1. Sang, H.; Zeng, J.; Qi, Y.; Mu, J.; Gan, F. Study on wheel wear mechanism of high-speed train in accelerating conditions. *Wear* **2023**, *516*, 204597.
2. Tao, G.; Wang, S.; Ren, D.; Li, J.; Wen, Z. Understanding and treatment of severe flange wear of metro train wheels. *Veh. Syst. Dyn.* **2022**, *61*, 2415-2431.
3. Bosso, N.; Magelli, M.; Zampieri, N. Simulation of wheel and rail profile wear: a review of numerical models. *Railway Eng. Sci.* **2022**, *30*, 403-436.
4. Li, Y.; Deng, J.; Wang, Y.; Liu, H.; Peng, L.; Zhang, H.; Liang, Y.; Feng, Q. The condition evaluation of bridges based on fuzzy BWM and fuzzy comprehensive evaluation. *Appl. Sci.* **2025**, *15*, 2904.
5. Wang, X.; Yang, J.; Wang, J.; Wang, Y.; Xu, G. An incentive factor-based dynamic comprehensive evaluation on a high-speed railway track. *Appl. Sci.* **2020**, *10*, 5546.
6. Zhang, G. Typical process capability analysis of small-batch production based on fuzzy matter-element. *Chin. J. Mech. Eng.* **2015**, *51*, 116-122.
7. Yi, L.; Zhao, J.; Yu, W.; Long, G.; Sun, H.; Li, W. Health status evaluation of catenary based on normal fuzzy matter-element and game theory. *J. Electr. Eng. Technol.* **2020**, *15*, 2373-2385.
8. Han, F.; Liu, Z.; Wang, C. Research on a comfort evaluation model for high-speed trains based on variable weight theory. *Appl. Sci.* **2023**, *13*, 3144.
9. Tang, J.; Wang, D.; Ye, W.; Dong, B.; Yang, H. Safety risk assessment of air traffic control system based on the game theory and the cloud matter element analysis. *Sustainability* **2022**, *14*, 6258.
10. Shu, J.; Ma, H.; Ding, W.; Jin, Z. Improved evidence fusion theory for the safety assessment of prestressed concrete bridges. *Buildings* **2024**, *14*, 1144.
11. Li, Q.; Fan, C. Evaluation of hydraulic-tunnel-lining durability based on ANP and cloud-model-improved matter-element theory. *Sustainability* **2022**, *14*, 11801.
12. Zhang, X.; Wu, Z.; Wang, H.; He, C.; Zhang, F.; Zhou, Y. Urban meteorological drought comprehensive index based on a composite fuzzy matter element-moment estimation weighting model. *iScience* **2024**, *27*, 110798.
13. Peng, H.; Chen, Y.; Shangguan, L.; Zhou, S.; Li1, Y.; Wang, Q. Evaluation of urban rail transit system planning based on integrated empowerment method and matter-element model. *Sustainability* **2025**, *17*, 4569.
14. Ran, Y.; He, Q.; Feng, Q.; Cui, J. High-accuracy on-site measurement of wheel tread geometric parameters by line-structured light vision sensor. *IEEE Access* **2021**, *9*, 52590-52600.
15. Pan, X.; Liu, Z.; Zhang, G. On-site reliable wheel size measurement based on multisensor data fusion. *IEEE Trans. Instrum. Meas.* **2019**, *68*, 4575-4589.
16. Zheng, F.; Zhang, B.; Gao, R.; Feng, Q. A high-precision method for dynamically measuring train wheel diameter using three laser displacement transducers. *Sensors* **2019**, *19*, 4148.
17. Liu, F.; Liang, L.; Hou, C.; Xu, G.; Liu, D.; Wang, L.; Chen, X.; Du, H. Measurement and evaluation of wheel profiles of a rail vehicle on an underfloor wheelset lathe. *Meas. Sci. Technol.* **2022**, *33*, 095010.
18. Chen, Y.; Li, Y.; Niu, G.; Zuo, M. Offline and online measurement of the geometries of train wheelsets: a review. *IEEE Trans. Instrum. Meas.* **2022**, *71*, 3523915.
19. Song, Z.; Guo, Z.; Zhou, F.; Tan, H.; Wang, X.; Zhang, P. Structured-light vision measurement approach for geometric parameters of wheelset under variable re-profiling working conditions. *IEEE Trans. Instrum. Meas.* **2025**, *74*, 5034212.

20. Li, H.; Li, L.; Yu, X.; Li, Z.; Sun, Y. Research on the influence of time-varying wear of wheel-rail profile on vehicle dynamic response. *Tribol. Int.* **2024**, *200*, 110095.
21. Fang, C.; Ding, Y.; Yan, H.; Chen, J.; Zhou, W.; Meng, X. Prediction and analysis of wheel flange wear on small curved track considering wheel-rail conformal and lubricated contact. *Wear* **2024**, *558*, 205569.
22. Muhamedsalih, Y.; Tucker, G.; Stow, J. Optimisation of wheelset maintenance by using a reduced flange wear wheel profile. *Proc. Inst. Mech. Eng. Part F-J. Rail Rapid Transit* **2022**, *237*, 253-265.
23. Saaty, T. L. A scaling method for priorities in hierarchical structures. *J. Math. Psychol.* **1977**, *15*, 234-281.
24. Zhang, J.; Li, M.; Zhang, J.; Yu, Y.; Liu, H.; Gao, H. A framework for condition assessment of communication tower with inspection data in Heilongjiang province, China. *Structures* **2025**, *75*, 108710.
25. Zhang, G.; Liu, G.; Lu, Z.; Yan, C.; Xu, L.; Gao, Q.; Zhou, Y. Evaluation method for health state of highway tunnel structure based on adaptive comprehensive weighting. *Eng. Fail. Anal.* **2024**, *163*, 108597.
26. Kim, J.; Kim, C.; Kim, G.; Kim, I.; Abbas, Q.; Lee, J. Probabilistic tunnel collapse risk evaluation model using analytical hierarchy process (AHP) and delphi survey technique. *Tunn. Undergr. Space Technol.* **2022**, *120*, 104262.
27. Xiao, K.; Tamborski, J.; Wang, X.; Feng, X.; Wang, S.; Wang, Q.; Lin, D.; Li, H. A coupling methodology of the analytic hierarchy process and entropy weight theory for assessing coastal water quality. *Environ. Sci. Pollut. Res.* **2022**, *29*, 31217-31234.
28. Jiang, W.; Wu, J.; Yang, Y.; Li, X.; Zhu, H. Health evaluation techniques towards rotating machinery: a systematic literature review and implementation guideline. *Reliab. Eng. Syst. Saf.* **2025**, *260*, 110924.
29. Chen, X.; Sun, J.; Liu, Z.; Zhang, G. Dynamic tread wear measurement method for train wheels against vibrations. *Appl. Optics* **2015**, *54*, 5270-5280.
30. Liu, S.; He, Q.; Fu, W.; Du, B.; Feng, Q. Multi-scale adaptive light stripe center extraction for line-structured light vision based online wheelset measurement. *Sensors* **2026**, *26*, 600.
31. He, Q.; Liu, S.; Fu, W.; Zhang, Z.; Feng, Q. High-accuracy on-line wayside wheelset size measurement based on multi-dimensional laser information fusion. **2025**, *254*, 117930.

Disclaimer/Publisher's Note: The statements, opinions and data contained in all publications are solely those of the individual author(s) and contributor(s) and not of MDPI and/or the editor(s). MDPI and/or the editor(s) disclaim responsibility for any injury to people or property resulting from any ideas, methods, instructions or products referred to in the content.